

# Synthesis, Characterization, and Reactivity of the Stable Iron Carbonyl Complex $[\text{Fe}(\text{CO})(\text{N4Py})](\text{ClO}_4)_2$ : Photoactivated Carbon Monoxide Release, Growth Inhibitory Activity, and Peptide Ligation

Casey S. Jackson,<sup>†</sup> Sara Schmitt,<sup>‡</sup> Q. Ping Dou,<sup>‡</sup> and Jeremy J. Kodanko<sup>\*,†</sup>

<sup>†</sup>Department of Chemistry, Wayne State University, 5101 Cass Avenue, Detroit, Michigan 48202, United States

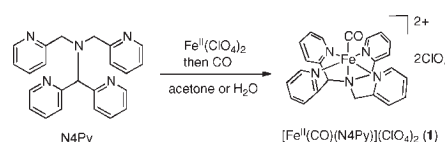
<sup>‡</sup>Developmental Therapeutics Program, Barbara Ann Karmanos Cancer Institute, Department of Pathology, School of Medicine, Wayne State University, Detroit, Michigan 48202, United States

**S** Supporting Information

**ABSTRACT:** Photoactivated carbon monoxide (CO) release by the iron carbonyl complex  $[\text{Fe}^{\text{II}}(\text{CO})(\text{N4Py})](\text{ClO}_4)_2$  (**1**) is described. Compound **1** is a low-spin ferrous complex that is highly stable and soluble in aerobic aqueous solutions. CO release was studied by the substitution of MeCN for CO, which displays saturation kinetics, and by the transfer of CO to deoxymyoglobin, which is slow in the dark but fast upon irradiation with UV light (365 nm). Compound **1** is active against PC-3 prostate cancer cells and shows potent photoinduced cytotoxicity. In addition, the iron carbonyl complex was attached to a short peptide toward the goal of tissue or cell-specific delivery.

The action of carbon monoxide (CO) as a heme poison was described over 80 years ago.<sup>1</sup> Long thought of as only a toxic gas, it took decades before the beneficial role of CO in physiology was acknowledged. Humans generate CO endogenously through catabolism of heme, which is catalyzed by the heme oxygenases.<sup>2</sup> Like nitric oxide, CO is now understood as both an essential signaling molecule and a potent pharmacological agent with beneficial effects when administered carefully.<sup>3</sup> Cell and animal studies have confirmed that CO acts as a vasodilator,<sup>4</sup> shows anti-inflammatory activity,<sup>5</sup> and can protect tissue from reperfusion injury.<sup>3,6</sup> The evaluation of CO in human clinical trials is ongoing.<sup>7</sup> However, it is difficult to administer CO as a gas in controlled amounts to tissues or organs specifically because of the rapid absorption of CO gas by hemoglobin (Hb) in the bloodstream. To address this issue, CO-releasing molecules (CORMs)<sup>8</sup> based on transition metals were developed that show benefits over CO gas, including kinetic control over CO release to reduce transfer to Hb, which can maximize the uptake of CO by cells.<sup>9</sup> Later derivatives addressed limitations with first-generation CORMs to maximize their solubility and stability in aqueous media.<sup>4,10</sup> However, the desire to deliver CO selectively to tumors and other tissues of interest has triggered the search for new CORMs.<sup>3</sup> In this Communication, we report a new iron carbonyl complex,  $[\text{Fe}^{\text{II}}(\text{CO})(\text{N4Py})](\text{ClO}_4)_2$  (**1**), which shows exceptional stability in aqueous media because of its slow release of CO. Furthermore, we demonstrate that CO release can be triggered rapidly by UV light, leading to potent, photoinitiated cytotoxicity against prostate cancer cells. We also demonstrate a method for attaching this CORM to a

## Scheme 1. Synthesis of **1**



peptide, toward the goal of achieving tissue- or cell-specific delivery with these complexes.

The carbonyl complex **1** can be synthesized as a solid from organic solvents or generated in situ in  $\text{H}_2\text{O}$  in a straightforward manner (Scheme 1). Treating the ligand N4Py with 1.0 equiv of  $\text{Fe}^{\text{II}}(\text{ClO}_4)_2$  in acetone under argon results in the formation of a reddish-orange solution. Bubbling of CO gas through the solution leads to a color change from reddish brown to light orange within minutes. Allowing the solution to stand under a CO atmosphere gives a light-orange precipitate that can be isolated as a solid in good yield (51%). Alternatively, the species  $[\text{Fe}^{\text{II}}(\text{CO})(\text{N4Py})]^{2+}$  can be formed in higher yield and in situ by treating the ligand N4Py with  $(\text{NH}_4)_2\text{Fe}^{\text{II}}(\text{SO}_4)_2 \cdot 6\text{H}_2\text{O}$  in deoxygenated  $\text{H}_2\text{O}$ , followed by bubbling of CO through the solution. This procedure gives **1** whose UV-vis and  $^1\text{H}$  NMR spectroscopic data match that of the solid. On the basis of the extinction coefficient for **1** in  $\text{H}_2\text{O}$ , a yield of 95% can be calculated when the complex is generated in this manner.

Compound **1** is diamagnetic in the solid state, implying a low-spin ferrous center ( $\chi_g < 0$ ). NMR spectroscopic analysis confirms that **1** retains its low-spin state in solution. Resonances from 9.2 to 5.2 ppm are observed in the  $^1\text{H}$  NMR spectrum in  $\text{D}_2\text{O}$  for **1**, are well-resolved, and are similar to those of the related species  $[\text{Fe}^{\text{II}}(\text{MeCN})(\text{N4Py})](\text{ClO}_4)_2$  (Figure S6 in the Supporting Information, SI). The IR spectrum for **1** shows an intense CO stretch ( $\nu_{\text{CO}}$ ) at  $2002\text{ cm}^{-1}$ , which is in the range for other low-spin ferrous carbonyls.<sup>11,12</sup> The UV-vis spectrum of **1** in  $\text{H}_2\text{O}$  shows two intense bands at 326 nm ( $\epsilon = 6900\text{ M}^{-1}\text{ cm}^{-1}$ ) (Figure S8 in the SI) and 390 nm ( $\epsilon = 4000\text{ M}^{-1}\text{ cm}^{-1}$ ). The mass spectrometry (MS) spectrum of **1** shows a prominent ion cluster with a major peak at  $m/z$  550.0568, along with a suitable isotopic distribution that matches that expected for the cationic cluster  $\{[\text{Fe}^{\text{II}}(\text{CO})(\text{N4Py})](\text{ClO}_4)\}^+$  (Figure S10 in the SI).

Received: April 1, 2011

Published: May 27, 2011

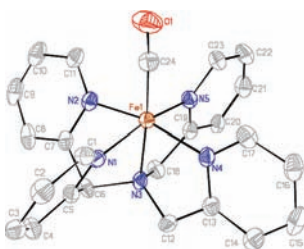


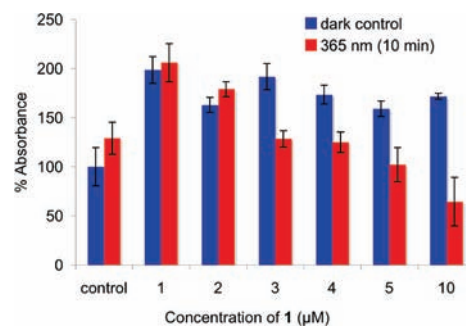
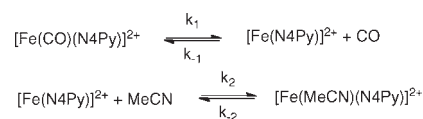
**Figure 1.** ORTEP diagram of the dication  $[\text{Fe}^{\text{II}}(\text{CO})(\text{N4Py})]^{2+}$  from compound **1**. Thermal ellipsoids are shown at 50% probability. Hydrogen atoms are omitted for clarity. Selected bond lengths (Å) and angles (deg): Fe1–C24, 1.783(4); C24–O1, 1.142(4); Fe1–N1, 1.978(3); Fe1–N2, 1.965(3); Fe1–N3, 1.973(3); Fe1–N4, 1.962(3); Fe1–N5, 1.964(3); Fe1–C24–O1, 176.4(4).

Orange plates of **1** suitable for X-ray crystallographic analysis were obtained by diffusing  $\text{Et}_2\text{O}$  into a solution of **1** in a mixture of MeOH and  $\text{H}_2\text{O}$  (20:1) under a CO atmosphere. Select data for **1** are described in Figure 1, and full tables can be found in the SI (Tables S1–S6). Fe1–C24 and C24–O1 bond lengths are 1.783(4) and 1.142(4) Å, respectively, and the Fe1–C24–O1 bond angle is  $176.4(4)^\circ$ , which are similar to those of the related complex  $[\text{Fe}^{\text{II}}(\text{CO})(\text{PaPy3})]^+$ .<sup>11</sup> Fe1–N distances range from 1.962(3) to 1.978(3) Å, which are in good agreement with the related low-spin iron(II) complex  $[\text{Fe}^{\text{II}}(\text{MeCN})(\text{N4Py})](\text{ClO}_4)_2$ .<sup>13</sup> Interestingly, these data confirm that the extent of back-bonding between the iron center and the carbonyl, which are indicated by the Fe–C bond length and  $\nu_{\text{CO}}$ , is not the only factor that determines the rate of CO loss in iron carbonyls of this type. The complex  $[\text{Fe}^{\text{II}}(\text{CO})(\text{PaPy3})]^+$  releases CO two orders of magnitude faster than **1** does in an aqueous buffer (vide infra), even though its Fe–C bond length is shorter [1.775(3) Å] and  $\nu_{\text{CO}}$  is smaller ( $1972\text{ cm}^{-1}$ ).<sup>11,12</sup>

Complex **1** shows remarkable stability in aqueous solution under aerobic conditions. When dissolved in aerobic water or phosphate buffer (PBS; 100 mM, pH 7.4) and left open to the atmosphere, the complex has a half-life of >1 day. To gain further insight into the CO-releasing behavior of **1**, the substitution of CO by MeCN and the transfer of CO to myoglobin (Mb) were studied.

Substitution of CO for MeCN in **1** slowly generates  $[\text{Fe}^{\text{II}}(\text{MeCN})(\text{N4Py})]^{2+}$  (Figure S1 in the SI).<sup>13</sup> Monitoring the reaction of **1** (1 mM) in  $\text{H}_2\text{O}$  with MeCN (10–1000 mM) by UV–vis spectroscopy reveals an isosbestic point at 339 nm, which is consistent with the conversion of CO to the MeCN-bound form without the formation of a long-lived intermediate. Kinetics of this substitution reaction demonstrate saturation behavior. When the initial rates of the reaction ( $dA/dt$ ) are plotted against the starting concentration of MeCN, rates saturate at approximately 200 mM MeCN and stay constant up to 1000 mM MeCN. These data are consistent with the kinetic sequence shown in Scheme 2, where at high concentrations of MeCN the loss of CO from **1** becomes the rate-determining step. The rate constant  $k_1$  (also known as  $k_{\text{CO}}$ ) was determined to be  $6.3(5) \times 10^{-6}\text{ s}^{-1}$  by conducting the substitution reaction using variable concentrations of **1** (see the SI for more details). This rate constant is almost 2 orders of magnitude lower than the  $k_{\text{CO}}$  values determined for iron carbonyls derived from related pentadentate ligands, illustrating the unique properties of the ligand N4Py in **1** and its slow release of CO.<sup>11,12</sup>

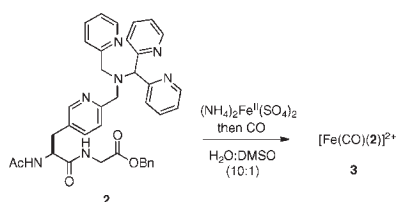
## Scheme 2. Substitution of MeCN for CO in **1**



**Figure 2.** Cytotoxicity of **1** on PC-3 prostate cancer cells. Cells were grown in the presence of **1** (1–10  $\mu\text{M}$ ) or  $\text{H}_2\text{O}$  (control) for 2 h and irradiated at 365 nm for 10 min (red) or left in the dark (blue). The cell viability was determined using the MTT assay, indicated as % absorbance relative to the dark control with no additive, after growing all cells in the dark for 8 h. Error bars represent the standard deviations of triplicate wells and are representative of three independent experiments. See the SI for more details.

In the dark, the transfer of CO from **1** to Mb is extremely slow (Figure S3 in the SI). Minimal transfer (<10%) of CO from **1** (120  $\mu\text{M}$ ) to Mb (60  $\mu\text{M}$ ) was observed after 4 h. However, upon irradiation of the sample of **1** and Mb with UV light (365 nm), full transfer of CO to Mb was observed within 10 min (Figure S2 in the SI).<sup>14,15</sup> The yield of Mb–CO was determined to be 92% based on a Mb–CO standard ( $\epsilon = 15\,400\text{ M}^{-1}\text{ cm}^{-1}$  at 540 nm).<sup>10</sup>

Although CO can protect normal tissues from injury, CO gas<sup>16</sup> and CORMs<sup>15</sup> have demonstrated cytotoxic effects in cancer cells.<sup>3</sup> We have confirmed that the iron carbonyl complex **1** shows potent photoinduced cytotoxicity in prostate cancer cells. PC-3 cells were incubated for 2 h in the presence of  $\text{H}_2\text{O}$  (control) or **1** (1–10  $\mu\text{M}$ ). Afterward, cells were irradiated for 10 min with 365 nm light or left in the dark as a control. After an additional 8 h of growing all cells in the dark, the cell viability was determined using the MTT assay (Figure 2). Control experiments with a water blank confirmed that irradiation alone has no effect on the cell viability within error. Cells treated with **1** in the dark did not show a concentration-dependent loss of viability over the concentration range of **1** surveyed (1–10  $\mu\text{M}$ ). However, irradiated cells showed a clear, concentration-dependent loss of viability between 1 and 10  $\mu\text{M}$ , with a maximum loss of viability at 10  $\mu\text{M}$ , which was 63% relative to the water control and 38% relative to cells grown in the dark with 10  $\mu\text{M}$  **1**. Thus, the cytotoxicity of **1** is photoinducible. The iron carbonyl complex **1** appears to be active against cancer cells in culture at lower concentrations than Mn- or Rh<sub>2</sub>-based photoactivated metal complexes.<sup>15,17</sup> However, these complexes were evaluated against different cancer cell lines, so it is difficult to make a direct comparison at this point. It is important to note that the high activity of **1** against PC-3 cells is due to the fact that photolysis of **1** releases two cytotoxic agents, CO and  $[\text{Fe}^{\text{II}}(\text{N4Py})]^{2+}$ , the latter of which shows growth inhibitory activity similar to

**Scheme 3. Synthesis of the Peptide-Ligated CORM**  
 $[\text{Fe}(\text{CO})_2(\mathbf{2})]^{2+}$ 


that of irradiated  $\mathbf{1}$  at a concentration of  $10 \mu\text{M}$  (Figure S4 in the SI).

Considering the observations that  $\mathbf{1}$  is stable, is soluble in aqueous media, and is slow to release CO in the presence of Mb (in the absence of light), this iron carbonyl has the potential to deliver CO to tissues or cells of interest in a biological setting. Therefore, we sought to demonstrate proof of principle that this complex could be attached to a peptide for creating cell- or tissue-specific reagents. Toward this goal, the known peptide  $\mathbf{2}$ ,<sup>18,19</sup> which contains the ligand N4Py bound to the Ala side chain of Ac-Ala-Gly-OBn, was treated with 1 equiv of  $(\text{NH}_4)_2\text{Fe}^{\text{II}}(\text{SO}_4)_2 \cdot 6\text{H}_2\text{O}$  followed by CO in a mixture of  $\text{H}_2\text{O}$  and dimethyl sulfoxide (DMSO) (10:1), resulting in the formation of compound  $[\text{Fe}^{\text{II}}(\text{CO})_2(\mathbf{2})]^{2+}$  ( $\mathbf{3}$ ; Scheme 3). Compound  $\mathbf{3}$  was characterized by UV-vis and  $^1\text{HMR}$  spectroscopies and by MS. The UV spectrum for  $\mathbf{3}$  in  $\text{H}_2\text{O}/\text{DMSO}$  (10:1) agrees well with the spectrum of  $\mathbf{1}$  (Figure S9 in the SI). Furthermore, the  $^1\text{H}$  NMR spectrum for  $\mathbf{3}$ , generated in  $\text{D}_2\text{O}/\text{DMSO}$  (10:1), shows resonances between 9.2 and 8.8 ppm, which are consistent with a diamagnetic, low-spin ferrous complex (Figure S7 in the SI). Within this spectrum, clear downfield shifts (ca. 0.5 ppm) for the pyridyl protons are noted with  $\mathbf{3}$ , as occurs with  $\mathbf{1}$  upon binding of the ligand to the  $\text{Fe}^{\text{II}}\text{CO}$  center. MS data for the complex generated in situ are consistent with the dication  $\mathbf{3}$ , showing a major peak at  $m/z$  363.6093, along with a suitable isotopic pattern (Figure S11 in the SI). Although we did not attempt to isolate the peptide-based CORM after its generation in situ, bubbling argon for 1 h through the aqueous solution did not cause this CORM to decompose, as judged by UV-vis spectroscopy, confirming that a stable aqueous solution of  $\mathbf{3}$  can be produced. It is important to note that the strategy for producing a peptide-based CORM described in this account differs from that of previous approaches where the metal carbonyl complex was preformed and then attached covalently to the peptide.<sup>20</sup> In the present study, treatment of the peptide-ligand conjugate in aqueous solution with metal salt followed by CO leads to the clean formation of the stable complex in aqueous media. We anticipate that the method of in situ generation, coupled with fast access to ligand derivatives,<sup>21</sup> will facilitate the rapid identification of suitable ligands for binding transition-metal carbonyls, including derivatives that release CO using longer, more biologically compatible wavelengths of light.

In conclusion, the synthesis, characterization, and reactivity of a new and exceptionally stable iron-based CORM  $\mathbf{1}$  have been described. Compound  $\mathbf{1}$  demonstrates attractive properties, such as strong CO binding, stability in aqueous solution, fast photolytic release of CO, photoinduced toxicity against cancer cells, and a suitable ligand structure for attachment to peptides. Synthesis and biological studies with  $\mathbf{1}$  and related peptide conjugates are now underway in our laboratory.

**ASSOCIATED CONTENT**

**S Supporting Information.** Experimental procedures, characterization data for  $\mathbf{1}$  and  $\mathbf{3}$ , including UV-vis,  $^1\text{H}$  and  $^{13}\text{C}$  NMR, IR, and MS spectra, kinetic analysis, and plots. This material is available free of charge via the Internet at <http://pubs.acs.org>.

**AUTHOR INFORMATION**
**Corresponding Author**

\*E-mail: [jkodanko@chem.wayne.edu](mailto:jkodanko@chem.wayne.edu).

**ACKNOWLEDGMENT**

J.J.K. thanks Mary Jane Heeg for crystallographic analysis, Nitinkumar Jabre for the synthesis of  $\mathbf{2}$ , and Wayne State University for its generous support of this research.

**REFERENCES**

- Haldane, J. B. S. *Biochem. J.* **1927**, *21*, 1068–1075.
- Tenhunen, R.; Marver, H. S.; Schmid, R. *Proc. Natl. Acad. Sci. U.S.A.* **1968**, *61*, 748–755.
- Motterlini, R.; Otterbein, L. E. *Nat. Rev. Drug Discovery* **2010**, *9*, 728–743.
- Foresti, R.; Hammad, J.; Clark, J. E.; Johnson, T. R.; Mann, B. E.; Friebe, A.; Green, C. J.; Motterlini, R. *Br. J. Pharmacol.* **2004**, *142*, 453–460.
- Sawle, P.; Foresti, R.; Mann, B. E.; Johnson, T. R.; Green, C. J.; Motterlini, R. *Br. J. Pharmacol.* **2005**, *145*, 800–810.
- Sandouka, A.; Fuller, B. J.; Mann, B. E.; Green, C. J.; Foresti, R.; Motterlini, R. *Kidney Int.* **2006**, *69*, 239–247.
- Mann, B. E. *Top. Organomet. Chem.*, **32**, 247–285.
- Motterlini, R.; Clark, J. E.; Foresti, R.; Sarathchandra, P.; Mann, B. E.; Green, C. J. *Circ. Res.* **2002**, *90*, e17–e24.
- Haas, K. L.; Franz, K. J. *Chem. Rev.* **2009**, *109*, 4921–4960.
- Zhang, W.-Q.; Atkin, A. J.; Thatcher, R. J.; Whitwood, A. C.; Fairlamb, I. J. S.; Lynam, J. M. *Dalton Trans.* **2009**, 4351–4358.
- Afshar, R. K.; Patra, A. K.; Bill, E.; Olmstead, M. M.; Mascharak, P. K. *Inorg. Chem.* **2006**, *45*, 3774–3781.
- Gonzalez, M. A.; Fry, N. L.; Burt, R.; Davda, R.; Hobbs, A.; Mascharak, P. K. *Inorg. Chem.* **2011**, *50*, 3127–3144.
- Roelfes, G.; Lubben, M.; Chen, K.; Ho, R. Y. N.; Meetsma, A.; Genseberger, S.; Hermant, R. M.; Hage, R.; Mandal, S. K.; Young, V. G., Jr.; Zang, Y.; Kooijman, H.; Spek, A. L.; Que, L.; Feringa, B. L. *Inorg. Chem.* **1999**, *38*, 1929–1936.
- Schatzschneider, U. *Inorg. Chim. Acta* **2011**, DOI: 10.1016/j.ica.2011.02.068.
- Niesel, J.; Pinto, A.; Peindy N'Dongo, H. W.; Merz, K.; Ott, I.; Gust, R.; Schatzschneider, U. *Chem. Commun.* **2008**, 1798–1800.
- Song, R.; Zhou, Z.; Kim, P. K. M.; Shapiro, R. A.; Liu, F.; Ferran, C.; Choi, A. M. K.; Otterbein, L. E. *J. Biol. Chem.* **2004**, *279*, 44327–44334.
- Aguirre, J. D.; Angeles-Boza, A. M.; Chouai, A.; Pellois, J.-P.; Turro, C.; Dunbar, K. R. *J. Am. Chem. Soc.* **2009**, *131*, 11353–11360.
- Jabre, N. D.; Hryhorczuk, L.; Kodanko, J. J. *Inorg. Chem.* **2009**, *48*, 8078–8080.
- Jabre, N. D.; Respondek, T.; Ulku, S. A.; Korostelova, N.; Kodanko, J. J. *J. Org. Chem.* **2010**, *75*, 650–659.
- Pfeiffer, H.; Rojas, A.; Niesel, J.; Schatzschneider, U. *Dalton Trans.* **2009**, 4292–4298.
- Jabre, N. D.; Korostelova, N.; Kodanko, J. J. *J. Org. Chem.* **2011**, *76*, 2273–2276.